Phytopathology Research

RESEARCH

Open Access

3-Ketoacyl-ACP synthase III FabH1 is essential for branched-chain DSF family signals in *Xanthomonas oryzae* pv. *oryzae*

Mingfeng Yan[1†], Yonghong Yu[2†], Lizhen Luo[1], Mei Huang[1], Yuanyin Zhang[1], Jingtong Su[1], Wenbin Zhang[1], Jincheng Ma[1], Zhe Hu[1*] and Haihong Wang[1*]

Abstract

The 3-ketoacyl-ACP synthase III (FabH), a key enzyme for bacteria growth, catalyses the last step of the initiation of bacterial fatty acid synthesis. Rice bacterial blight is caused by the pathogen *Xanthomonas oryzae* pv. *oryzae* (*Xoo*), which is widely studied as a model bacterium. Bioinformatics analysis showed that the *X. oryzae* pv. *oryzae* PXO99A genome encodes three FabH homologous proteins with unknown functions. In this study, we found that only PXO_02706 (*fabH1*) encodes a functional FabH, the key enzyme in the production of branched-chain fatty acid, which is essential for the branched-chain diffusible signal factor family signals in *Xoo*. Interestingly, we found that FabH1 is not essential for fatty acid biosynthesis in *Xoo*. Pathogenicity analysis showed that loss of *fabH1* caused a significant decrease in virulence of *Xoo*. Genetic and phenotypic analyses revealed that *fabH1* plays a key role in multiple *Xoo* virulence-related activities, including exopolysaccharide (EPS) production, biofilm formation, motility, and resistance to environmental stresses.

Keywords *Xanthomonas oryzae* pv. *oryzae*, 3-Ketoacyl-ACP synthases III, Fatty acid biosynthesis, Branched-chain DSF-family signals, Pathogenesis

Background

Xanthomonas oryzae pv. *oryzae* (*Xoo*) is among the top ten most devastating plant pathogenic bacteria, and is the causal agent of rice bacterial leaf blight disease (Nino-Liu et al. 2006; Mansfield et al. 2012). During blight infection, *Xoo* activates the diffusible signal factor (DSF) family quorum sensing (QS) signals, which globally regulates pathogenicity (He and Zhang 2008; He et al. 2010). Previous studies have shown that DSF-family signal components, such as DSF (*cis*-11-methyl-2-dodecenoic acid), CDSF (*cis*, *cis*-11-methyldodeca-2,5-dienoic acid), IDSF (*cis*-10-methyl-2-dodecenoic acid), and BDSF (*cis*-2-dodecenoic acid), regulate virulence factor production in *Xanthomonas* spp. by the *rpf* gene cluster, including *rpfF*, *rpfB*, *rpfC*, and *rpfG* that encode DSF synthase, acyl-CoA ligase, sensor, and response regulator, respectively (Slater et al. 2000; Andrade et al. 2006; He et al. 2010; An et al. 2014; Bi et al. 2014; Wang et al. 2016). 3-Hydroxyacyl-ACPs are the precursors of DSF-family signal components (Zhou et al. 2015, 2017b). Previous studies showed that 3-hydroxyacyl-ACPs are generated by the fatty acid synthesis (FAS) pathway (Zhou et al. 2015).

[†]Mingfeng Yan and Yonghong Yu contributed equally to this work.

*Correspondence:
Zhe Hu
zhehu@scau.edu.cn
Haihong Wang
wanghh36@scau.edu.cn
[1] Guangdong Provincial Key Laboratory of Protein Function and Regulation in Agricultural Organisms, College of Life Sciences, South China Agricultural University, Guangzhou 510642, China
[2] Guangdong Food and Drug Vocational College, Guangzhou 510520, China

FAS is important for all organisms (White et al. 2005; Zhang and Rock 2008). Fatty acids (FAs) are not only required for biosynthesis of cell membrane phospholipids (Zhang and Rock 2008), but also are the intermediates of the biosynthesis of many bioactive substances, such as biotin (Lin and Cronan 2011), rhamnolipids (Du et al. 2017), lipoic acid (Cronan et al. 2005), lipid A (Zhang and Rock 2008), and QS signalling molecules including DSFs and N-acyl-homoserine lactones (AHLs) (Zhou et al. 2015; Huang et al. 2016). De novo FA synthesis in bacteria is catalysed by the type II fatty acid synthesis system (FAS II), which is composed of a series of small independent enzymes (Cronan and Rock 2008). Intermediates in FAS II are shuttled from between biosynthesis enzymes by a small highly acidic acyl carrier protein (ACP) (Campbell and Cronan 2001; Cronan and Rock 2008). Fatty acid biosynthesis begins with the conversation of acetyl-CoA into malonyl-CoA by acetyl-CoA carboxylase AccABCD (Davis et al. 2000). Malonyl-CoA:ACP transacylase (FabD) then transfers malonyl-CoA to malonyl-ACP (Magnuson et al. 1992). Malonyl-ACP further combines with an acetyl-CoA group in the first condensation reaction, catalysed by 3-ketoacyl-ACP synthetase III (KAS III), to form 3-ketobutyryl-ACP (Cronan and Rock 2008). KAS III is a key enzyme for bacterial fatty acid biosynthesis that determines the type and amount of fatty acids in different bacteria (Marrakchi et al. 2002; White et al. 2005). In *Escherichia coli*, FabH functions as a KAS III that preferentially utilises acetyl-CoA and malonyl-ACP to synthesize the straight-chain fatty acids (SCFAs) (Heath and Rock 1995), whereas its counterparts in many Gram-positive bacteria, such as *Bacillus subtilis*, selectively catalyse branched-chain acyl-CoA and malonyl-ACP to generate branched-chain fatty acids (BCFAs) (Choi et al. 2000).

Xoo has a complex fatty acid profile which is comprised of saturated SCFAs, unsaturated fatty acids (UFAs), and BCFAs (Vauterin et al. 1996), but the FAS pathway in *Xoo* is less known. In the present study, we found that PXO_02706 (*fabH1*) is the only functional KAS III. It plays a key role in the biosynthesis of BCFAs and branched-chain DSF family signal components in *Xoo.* Pathogenicity analysis showed that the *fabH1* gene was required for full virulence of *Xoo* on rice. Knockout of *fabH1* resulted in a significant decrease in the production of several pathogenicity-related virulence activities, including exopolysaccharide (EPS) production, biofilm formation, motility, and resistance to environmental stresses.

Results

Only *fabH1* can complement the growth of *Ralstonia solanacearum fabH* deletion mutant

According to the genome annotation, the *Xanthomonas oryzae* pv. *oryzae* PXO099A genome contains three putative *fabH* genes (Fig. 1a), the *fabH1* (PXO_02706), *fabH2* (PXO_00990), and *fabH3* (PXO_03957). All three putative FabHs contain a Cys-His-Asn catalytic triad (Fig. 1b), implying that they may function in initiation of fatty acid synthesis. The *fabH1* gene is located within a cluster of fatty acid synthesis genes (*plsX-fabH1-fabD-fabG-acpP-fabF*). About 60.1% of the residues of FabH1 protein are identical to the orthologous of *E. coli. fabH2* and *fabH3*, encoding 3-ketoacyl-ACP synthase III (KAS III) candidates, are located in a separate operon that is far away from the above-mentioned genes. FabH2 and FabH3 share only 27.1% and 28.6% identity with *E. coli* orthologous, respectively.

To explore whether these proteins function in fatty acid synthesis initiation, the plasmids pMF1 (*fabH1*), pMF2 (*fabH2*), and pMF3 (*fabH3*) were transformed into the *R. solanacearum fabH* deletion mutant Δ*RsfabH*, which does not grow on BG medium without octanoic acid supplementation (Mao et al. 2015). The Δ*RsfabH* harbouring plasmid pMF1 grew well in the absence of octanoic acid, whereas pMF2 and pMF3 could not rescue the growth of Δ*RsfabH* under the same conditions (Fig. 1c). To investigate the functions of FabH1 in fatty acid synthesis, the fatty acids in the resulting strains were determined by gas chromatography–mass spectrometry (GC–MS). *R. solanacearum* GMI1000 does not produce branched-chain fatty acids (BCFAs) (Table 1). However, the Δ*RsfabH* mutant harbouring pMF1 contained ~ 48.8% BCFAs, including *iso*-$C_{15:0}$, *iso*-$C_{17:0}$, and *antesio*-$C_{17:0}$ (Table 1). These results indicate that only *fabH1* encodes a functional KAS III, enabling the initiation of fatty acid biosynthesis in vivo.

Analysis of *Xoo* FabH activities in vitro

In order to perform a direct in vitro assay of *Xoo* FabHs' activities, the recombinant proteins were expressed and purified from *E. coli* (Fig. 2a). Various *E. coli* fatty acid biosynthetic proteins, including FabD, FabB, FabG, FabA, FabI, holo-ACP, and *Vibrio harveyi* acyl-ACP synthetase (AasS), were also purified using the same method.

To investigate the functions of *Xoo* FabHs, the initial reaction was reconstructed by adding of acetyl-CoA, malonyl-ACP, FabHs, and *E. coli* fatty acid synthesis enzymes mentioned above, and the products were analysed by conformationally sensitive gel electrophoresis. *E. coli* FabH could condense acetyl-CoA and malonyl-ACP to generate 3-oxobutyryl-ACP, and finally produce

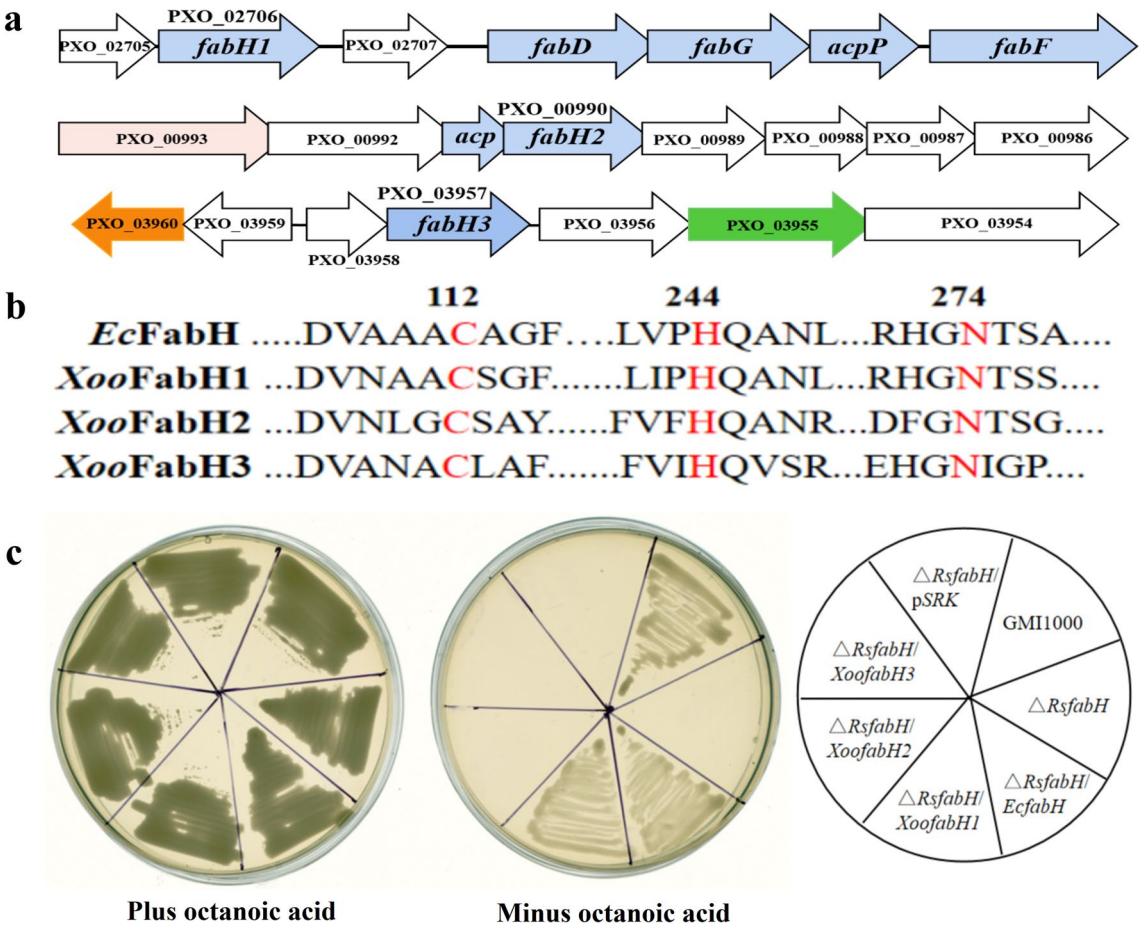

Fig. 1 FabH homologue coding genes and the complementation of *R. solanacearum fabH* knockout strain Δ*RsfabH*. **a** Loci of *XoofabHs*. The *fabH1* locus is similar to the *E. coli fabH* locus. **b** Structure-based amino acid alignments of FabH homologues from *Xoo*. Residues that constitute the His-Asn-Cys catalytic triad are highlighted (Cys112, His244, and Asn274 in *Ec*FabH). **c** *R. solanacearum fabH* knockout strain Δ*RsfabH* carrying the plasmid of pMF1(*fabH1*) was grown on BG medium in the absence of octanoic acid

Table 1 Fatty acid composition of Δ*RsfabH* complementary strains and *Xoo* mutant strains

Strain	n-$C_{14:0}$	*iso*-$C_{15:0}$	n-$C_{16:0}$	n-$C_{16:1}$	*iso*-$C_{17:0}$	*anteiso*-$C_{17:0}$	n-$C_{18:0}$	n-$C_{18:1}$
GMI1000%	1.5 ± 0.3	–	29.5 ± 2.7	11.6 ± 1.4	–	–	22.4 ± 1.6	32.1 ± 3.3
Δ*RsfabH/XoofabH1*%***	1.0 ± 0.3	37.8 ± 2.3	9.2 ± 1.1	14.8 ± 2.1	6.4 ± 0.2	4.6 ± 0.6	18.7 ± 1.2	7.5 ± 1.5
Xoo%	1.26 ± 0.15	7.72 ± 0.05	41.64 ± 2.2	30.9 ± 2.72	8.72 ± 0.84	–	8.3 ± 1.11	1.46 ± 0.09
Δ*fabH1*%***	1.79 ± 0.3	0.17 ± 0.04	48.79 ± 0.92	37.37 ± 2.53	–	–	9.8 ± 1.94	2.08 ± 0.72
Δ*fabH2*%	1.14 ± 0.2	6.47 ± 0.1	39.39 ± 1.9	32.13 ± 0.3	9.22 ± 0.4	–	9.65 ± 1.3	2.01 ± 0.32
Δ*fabH3*%	1.26 ± 0.6	8.11 ± 1.7	41.7 ± 1.8	29.35 ± 1.2	8.61 ± 0.6	–	9.33 ± 1.6	1.63 ± 0.2
Δ*fabH1/fabH1*%*	1.61 ± 0.38	6.92 ± 2.25	38.97 ± 1.56	28.51 ± 0.58	13.66 ± 1.01	–	7.91 ± 2.53	2.41 ± 0.91

Total lipids were extracted and transesterified to fatty acid methyl esters, and products were identified by GC–MS. Values are percentages of total fatty acids and are the mean ± standard deviations of three independent experiments. Pair-wise comparisons were made between the Δ*RsfabH* complementary strains and wild-type strain GMI1000, and the wild-type strain PXO99A and mutant strains or complemented strains, by Student's *t*-test (***$P < 0.001$; **$P < 0.01$; *$P < 0.05$). n-$C_{14:0}$, tetradecanoic acid; *iso*-$C_{15:0}$, 13-methyl-tetradecanoic acid; n-$C_{16:1}$, *cis*-9-hexadecenoic acid; n-$C_{16:0}$, hexadecanoic acid; *iso*-$C_{17:0}$, 15-methyl-hexadecanoic acid; *anteiso*-$C_{17:0}$, 14-methyl-hexadecanoic acid; n-$C_{18:0}$, octadecanoic acid; n-$C_{18:1}$, *cis*-11-octadecenoic acid

butyryl-ACP (Fig. 2b, lane 3). Interestingly, FabH1 could produce longer chain products, namely hexanoyl-ACP and octanoyl-ACP (Fig. 2b, lane 4). These results suggest that FabH1 not only catalyses the initiation reaction, but also functions in the elongation cycle, where it utilizes acyl-ACP and malonyl-ACP to generate $C_{6:0}$-ACP

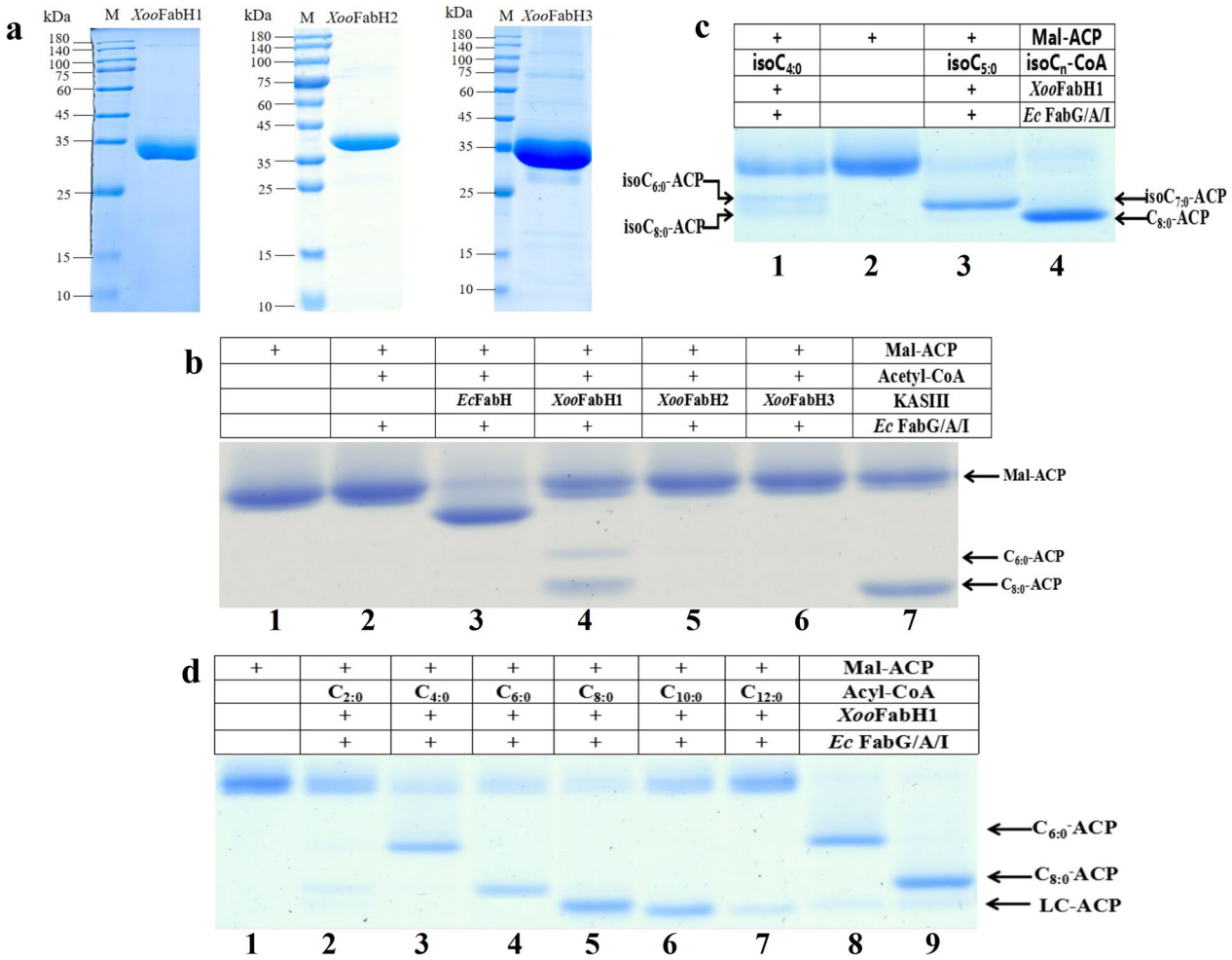

Fig. 2 *Xoo*FabH1 encodes a 3-ketoacyl-ACP synthase III to initiate FASII. **a** SDS-PAGE analysis of purified *Xoo*FabHs. **b** Condensation of malonyl-ACP with acetyl-CoA by purified *Ec*FabH (lane 3), *Xoo*FabH1 (lane 4), *Xoo*FabH2 (lane 5), or *Xoo*FabH3 (lane 6). The migration positions of octanoyl-ACP ($C_{8:0}$-ACP, lane 7) on gel are shown. **c** Condensation of malonyl-ACP with isobutyryl-CoA (lane 1) or isovaleryl-CoA (lane 3) by purified FabH1. The migration positions of octanoyl-ACP ($C_{8:0}$-ACP, lane 4) on gel are shown. **d** Condensation of malonyl-ACP with acyl-CoAs ($C_{4:0}$-CoA to $C_{12:0}$-CoA) by purified *Xoo*FabH1 (lane 3 to lane 7). The migration positions of hexanoyl-ACP ($C_{6:0}$-ACP, lane 8) and octanoyl-ACP ($C_{8:0}$-ACP, lane 9) on gel are shown. The initiation fatty acid synthesis was reconstructed using a combination of *E. coli* FabZ, FabG, FabI, and *Xoo* FabH1 with NADH, and NADPH as cofactors, and malonyl-ACP plus acetyl-CoA or isoacetyl-CoA as substrates

or $C_{8:0}$-ACP. However, adding of FabH2 or FabH3 in the reaction system failed to produce any new bands (Fig. 2b, lanes 5 and 6), indicating that neither *fabH2* nor *fabH3* encodes KAS III.

To investigate the substrate specificity of FabH1, branched-chain acyl-CoAs (isobutyryl-CoA or isovaleryl-CoA) were tested. The results showed that FabH1 used branched-chain acyl-CoAs, isobutyryl-CoA, or isovaleryl-CoA as a primer to initiate fatty acid synthesis (Fig. 2c, lanes 1 and 3). The activities of FabH1 to utilise straight-chain acyl-CoAs (butyryl-CoA, hexanoyl-CoA, octanoyl-CoA, decanoyl-CoA, or dodecanoyl-CoA) as substrates were also tested, where each of the acyl-CoAs could be converted to the longer acyl-ACPs by FabH1 (Fig. 2d). We also found that FabH2 and FabH3 failed to elongate any of the straight-chain or branched-chain acyl-CoAs (Additional file 1: Figure S1). Thus, only FabH1 functions in fatty acid biosynthesis.

FabH1 is not essential for growth, but is essential for BCFA biosynthesis in *Xoo*

The physiological functions of FabHs were further explored via gene deletion mutants. Using suicide plasmids carrying in-frame gene deletions to disrupt *fabH1*, *fabH2*, or *fabH3*, single-gene knockout of each of the three putative *fabH* genes in the PXO99A strain was

achieved. Deletion of any of the *fabH* genes did not affect their growth on NA medium, suggesting that none of the genes are essential for growth of *Xoo* (Additional file 1: Figure S2).

To test whether FabH1 has 3-ketoacyl-ACP synthetase III activity in vivo, we analysed the fatty acid composition of Δ*fabH1*, Δ*fabH2*, and Δ*fabH3* by GC–MS. The FA profile of the wild type (WT) strain *Xoo* PXO99A included iso-BCFAs, anteiso-BCFAs, saturated straight-chain fatty acids (SCFAs), and unsaturated SCFAs (Table 1). In *Xoo* PXO99A, anteiso-BCFAs were only observed with trace amounts, and iso-BCFAs were the predominant BCFAs, including *iso*-$C_{15:0}$ (7.72 ± 0.05%) and *iso*-$C_{17:0}$ (8.72 ± 0.84%). The predominant FAs in *Xoo* were SCFAs, mainly the n-$C_{16:0}$ (41.64 ± 2.2%) and n-$C_{16:1}$ (30.9 ± 2.27%). Deletion of *fabH1* resulted in the loss of BCFAs (< 1%), while the composition of n-$C_{16:0}$ and n-$C_{16:1}$ increased up to 48.79 ± 0.92% and 37.37 ± 2.53%, respectively (Table 1). Biosynthesis of BCFAs could be restored to WT levels by introducing a single copy of *fabH1* (Table 1). We also analysed the FA composition in Δ*fabH2* and Δ*fabH3*, and no significant changes were found in either Δ*fabH2* or Δ*fabH3*. Thus, FabH1 is likely responsible for BCFA biosynthesis, and FabH2 and FabH3 might not be involved in fatty acid biosynthesis.

FabH1 is required for biosynthesis of branched-chain DSF family signal components in *Xoo*

In this study, we confirmed that *fabH1* deletion disrupted BCFA biosynthesis. Therefore, we believe that deletion of *fabH1* would result in the defective branched-chain DSF family signal component biosynthesis. To test this hypothesis, DSF family signal production was examined in DSF high-yielding Δ*rpfBC*-derived strains using high-performance liquid chromatography (HPLC) (Zhou et al. 2017a). Both Δ*rpfBCfabH1* and Δ*rpfBCfabH1/fabH1* complementary strains were constructed. The results showed that deletion of *fabH1* significantly decreased IDSF production. BDSF production was not affected, while CDSF and DSF signal components were not detectable in the mutant strain (Fig. 3). As expected, the introduction of a single copy of *fabH1* restored CDSF, IDSF, and DSF production to WT levels (Fig. 3). These results indicate that precursors of DSF family signals are derived from intermediate metabolites of the FAS pathway, and FabH1 is the key enzyme in the production of branched-chain DSF family signals in *Xoo*.

fabH1 is required for full virulence of *Xoo*

Previous studies showed that DSF promotes functions required for attachment and biofilm formation, and

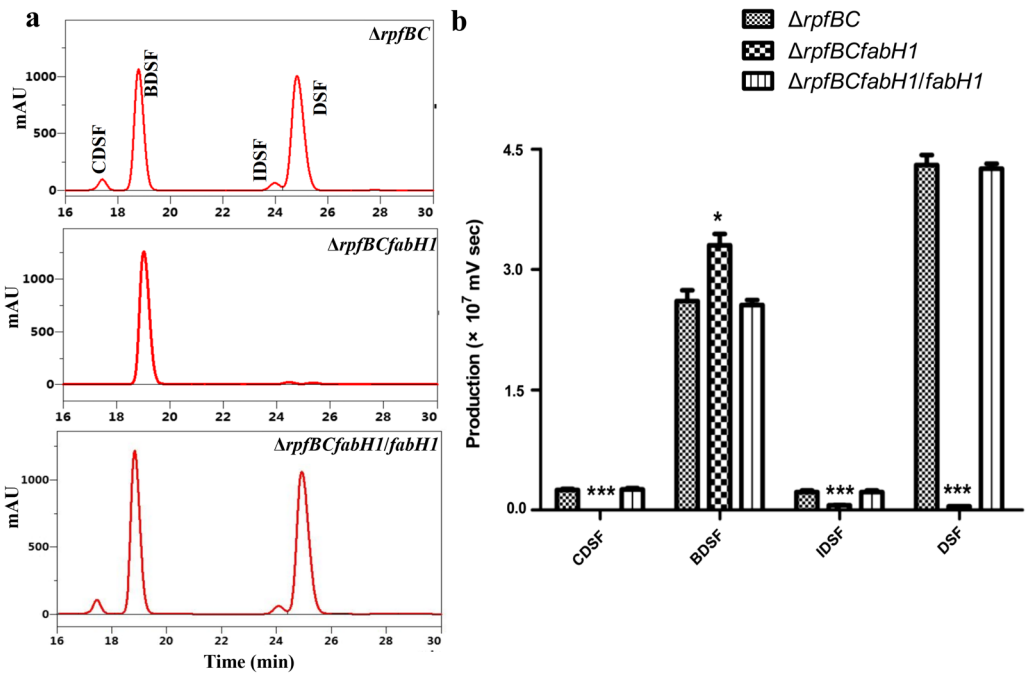

Fig. 3 Diffusible signal factor (DSF)-family signal components produced by *fabH1* deletion mutant. **a** DSF signal components produced by *fabH1* deletion mutant that was grown in 50 mL NA medium at 30°C for 24 h were collected and detected by HPLC. **b** The relative DSF-family signal component levels at 24 h after inoculation. The amounts of signal molecules were calculated based on peak areas. Values are the means ± SDs from three independent experiments. The asterisks above the error bars indicate significant differences compared with the wild-type strain (***$P < 0.001$). All experiments were repeated three times with similar results

suppresses motility in *Xoo* (Torres et al. 2007; He and Zhang 2008; Zhu et al. 2011; Rai et al. 2012). Our current results showed that Δ*fabH1* was defective in branched-chain DSF family signal component biosynthesis. To evaluate whether *fabH1* contributes to *Xoo* virulence, a leaf-clipping virulence assay using susceptible rice plants (*Oryza sativa* L. *japonica* cv. Nipponbare) was conducted. The WT PXO99A strain caused an average lesion length of 10.7 ± 1.4 cm at 2 weeks post inoculation (Fig. 4). The Δ*fabH1* mutant infection resulted in a significantly reduced lesion length in all infected leaves (5.6 ± 1.0 cm), and the complementary strain Δ*fabH1*/*fabH1* maintained similar pathogenicity to the WT strain (Fig. 4). These results suggest that deletion of *fabH1* resulted in the significantly decreased pathogenicity of *Xoo* on rice leaves.

To understand why Δ*fabH1* showed reduced pathogenicity on rice plants, we evaluated several pathogenicity-related virulence factors produced by *Xoo* strains. Previous reports have demonstrated that DSF positively regulates EPS production and biofilm formation (Slater et al. 2000; Torres et al. 2007). Production of EPS was therefore investigated, and the amounts of EPS produced by WT PXO99A, Δ*fabH1*, and the complementary strain Δ*fabH1*/*fabH1* were 8.1 ± 0.28, 2.0 ± 0.1, and 7.9 ± 0.1 mg/mL, respectively (Fig. 5a). The amount of EPS produced by Δ*fabH1* was significantly lower than that of the WT strain, but the amount of EPS produced by Δ*fabH1*/*fabH1* was not statistically different from that produced by the WT strain (Fig. 5a).

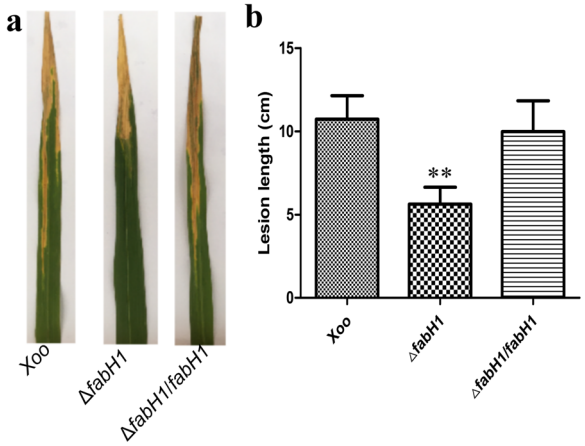

Fig. 4 *fabH1* is required for the full virulence of *Xoo*. **a** Lesion lengths on 5 weeks old rice leaves inoculated with the *Xoo* strains after 2 weeks. **b** Calculated lesion lengths were recorded from the *Xoo* strains inoculated rice leaves in a growth chamber. Values are the means ± SDs from three independent experiments. The asterisks above the error bars indicate significant differences compared with the wild-type strain ($^{**}P < 0.01$). All experiments were repeated three times with similar results

Next, the crystal violet assay was performed to monitor the formation of biofilm by the Δ*fabH1* mutant. The results showed that deletion of *fabH1* decreased biofilm production to 66.5% in the WT strain (Fig. 5b). DSF-mediated QS systems not only control the production of many virulence factors in *Xoo*, but are also involved in the regulation of *Xoo* motility (Rai et al. 2012). Thus, we evaluated the motility ability of *Xoo* strains in semisolid motility agar. The results showed that the diameter of the swimming zone of the WT strain was 2.06 ± 0.3 cm, while that of Δ*fabH1* was only 0.81 ± 0.18 cm. In addition, the diameter of the swarming zone of the WT strain was 1.99 ± 0.11 cm, while the swarming zone of Δ*fabH1* was only 0.88 ± 0.05 cm. These results indicated that deletion of *fabH1* reduced *Xoo* swimming and swarming, and the complementary strain restored their motility ability to WT levels (Fig. 5c, d). The amylase and cellulase production assays showed that the Δ*fabH1* mutant produced WT levels of these three extracellular enzymes, suggesting that it is not involved in regulating the production of extracellular enzymes in *Xoo* (Fig. 5e).

The growth of *Xoo*-derived strains on NA medium was investigated under various environmental challenges, including H_2O_2, the anionic surfactant sodium dodecyl sulphate (SDS), low pH, and high salt concentration. The results showed that 1.5% NaCl, 0.055 mM H_2O_2, 0.01% SDS, pH 5.5, and pH 8.0 differentially affected Δ*fabH1* strain growth, indicating that Δ*fabH1* was sensitive to many environmental stresses mentioned above. The *fabH1* complementary strain grew well on medium containing 1.5% NaCl, 0.055 mM H_2O_2, or 0.01% SDS, but Δ*fabH1/fabH1* only partially restored growth at pH 5.5 or pH 8.0 (Fig. 5f). Taken together, these findings indicate that *fabH1* positively regulated EPS production, biofilm formation, motility, and resistance to environmental stresses.

Discussion

Xoo, the pathogen causing bacterial leaf blight, affects the quality and yield of rice worldwide (Nino-Liu et al. 2006; He et al. 2010). Pathogenicity of *Xoo* is extensively regulated by the DSF-based quorum sensing system (Zhou et al. 2017a), while DSF signals are initiated by the intermediates of the FAS system (Zhou et al. 2015), which is considered as an attractive target for antibacterial agent development (Heath et al. 2001). However, the fatty acid synthesis pathway in *Xoo* is poorly understood. FabH is a key enzyme in fatty acid synthesis, hence our study focused on elucidating the functions of FabH in *Xoo*.

Although three genes are annotated as FabH-coding candidates in the genome of *Xoo*, only *fabH1* could rescue the growth of *R. solanacearum* Δ*RsfabH* (Fig. 1c), and enables the mutant to produce large quantities of

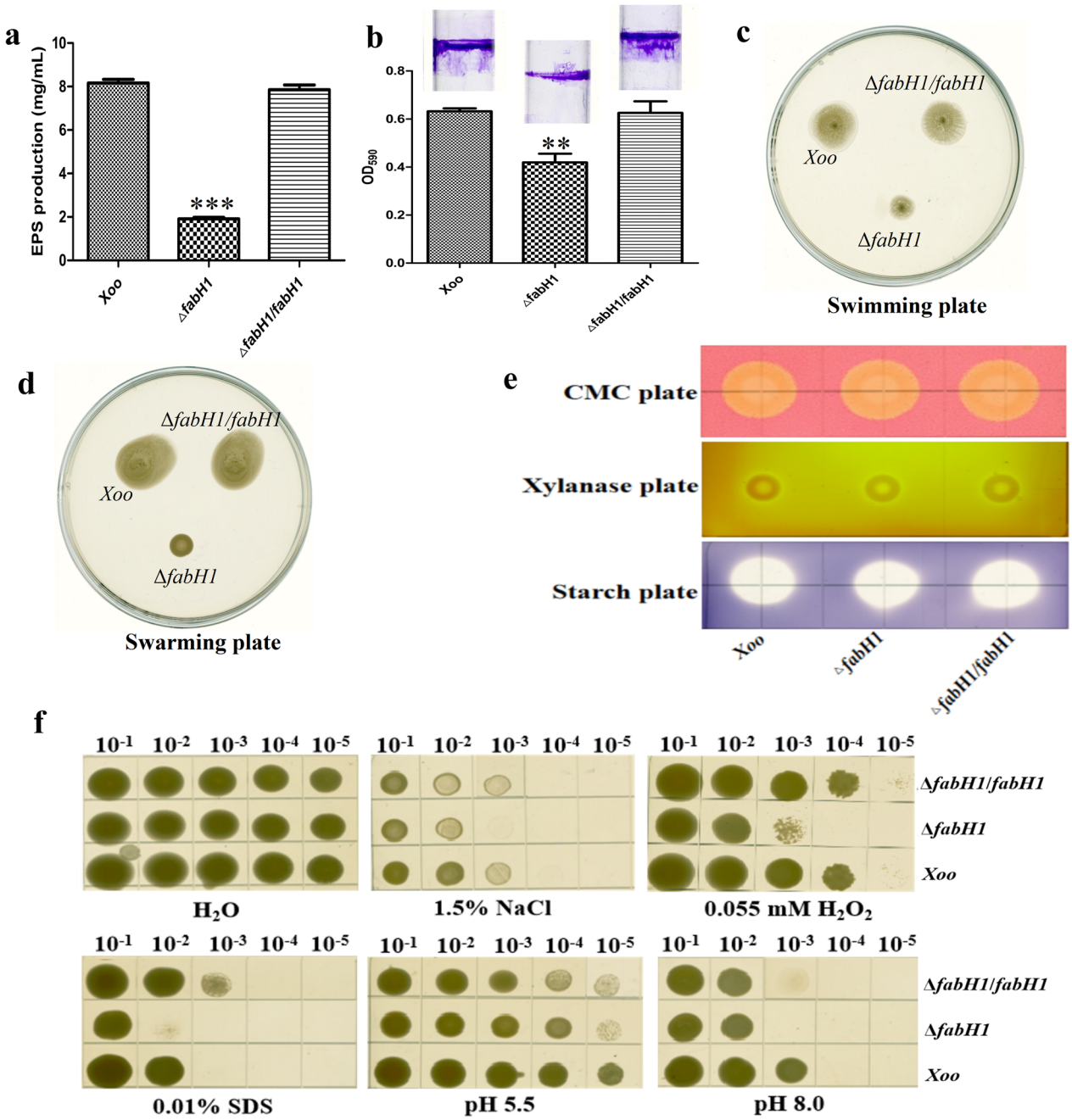

Fig. 5 Phenotypic changes of EPS production, biofilm formation, motility, resistance to environmental stress in *fabH1* deletion mutant. **a** Production of extracellular polysaccharide (EPS) in *Xoo* strains. **b** Biofilm production and its quantification of the *Xoo* strains on polystyrene tubes. **c, d** Typical bacterial halos, formed on semisolid 0.3% and 0.5% agar plates after incubation at 30°C for 2 days. **e** Relative activities of extracellular enzymes (cellulase and amylase) produced by *Xoo* strains on NA plates. **f** The *Xoo* strains were spotted onto NA plates containing increasing levels of NaCl, SDS, pH or H_2O_2. Values are the means ± SDs from three independent experiments. The asterisks above the error bars indicate significant differences compared with the wild-type strain ($^{**}P < 0.01$). All experiments were repeated three times with similar results

BCFAs (Table 1). Moreover, FabH1 showed catalytic activity to various substrates in vitro, but the activities of FabH2 and FabH3 were not detected (Fig. 2). The Δ*fabH1* mutant showed a similar growth phenotype as the WT strain (Additional file 1: Figure S2), but BCFA production was abolished (Table 1). Moreover, DSF was almost undetectable, but similar amounts of BDSFs were produced by deleting of *fabH1* (Fig. 3). FabH1 is the key

enzyme in the production of BCFAs and branched-chain DSF family signal components in *Xoo* (Fig. 6). Deletion of *fabH1* also caused a significant decrease in pathogenicity on host plants, and the reduced production of virulence-related factors and resistance to stresses may collectively contribute to the attenuated pathogenicity (Figs. 4, 5).

Protein sequence alignment analysis showed that FabH2 and FabH3 shared only 27.1% and 28.6% identity with *E. coli* FabH, respectively, implying that FabH2 and FabH3 may not possess 3-ketoacyl ACP synthesase III activities. The hypothesis was confirmed in the complementary experiments and in vitro enzymatic analysis. The mutant Δ*fabH2* and Δ*fabH3* displayed similar fatty acid profiles, and showed a same growth pattern with wild-type strain, indicating that neither *fabH2* nor *fabH3* is essential for fatty acid synthesis and bacterial growth. However, further study is necessary to explore the functions of FabH2 and FabH3.

Compared with SCFAs, BCFAs contain an additional methyl group, and are essential in maintaining membrane fluidity in many Gram-positive bacteria (Choi et al. 2000; Li et al. 2005; Singh et al. 2009). However, the *fabH1* deletion mutant did not produce BCFAs (Table 1), but its growth curve was similar to that of the WT strain (Additional file 1: Figure S2), implying that BCFAs were not essential for growth under the tested conditions. Similar results were also found in our previous study with the other phytopathogen *Xanthomonas campestris* pv. *campestris* (*Xcc*) (Yu et al. 2016). Only trace amounts of BCFAs (< 1%) were detected when *XccfabH* was replaced by *E. coli fabH* (Yu et al. 2016). We thus speculate that BCFAs are not important for the growth in the *Xanthomonas* genus. One plausible explanation is that both *Xoo* and *Xcc* produce a complex composition of FAs, including BCFAs, SCFAs, and UFAs, in which UFAs can replace the functions of BCFAs. The increased percentage of UFAs in the *fabH1* deletion mutant is consistent with this hypothesis. However, whether UFAs in *Xoo* are essential for growth is not clear, and our group is attempting to answer this question by exploring the biosynthetic mechanism of UFAs in *Xoo*.

Many studies have showed that KAS III is the sole enzyme that catalyses the condensation step in the initiation of the FAS II system (Lin and Cronan 2011; Mao et al. 2015), hence the *fabH* gene is essential for bacterial growth (Lai and Cronan 2003; Parsons and Rock 2013), and is a promising target for antibacterial drug discovery (Marrakchi et al. 2002). However, our study indicated that the Δ*fabH1* mutant grew well on nutrition-rich media (Additional file 1: Figure S2), indicating that *fabH1* is not essential for bacterial growth in *Xoo*. The opposite result was found in studies on *Xcc*, in which no *fabH* deletion mutant was isolated, but the *E. coli fabH* replacement strain *Xcc fabH::EcfabH* was constructed, suggesting that *Xcc fabH* is an essential gene for *Xcc* growth (Yu et al. 2016). One possible reason for this observation is that another 3-ketoacyl-ACP synthase (FabB or FabF) may partially compensate for the activity of FabH in the deletion mutant. Indeed, several reports showed that overproduction of FabB or FabF can bypass the initiation step in FAS II (Morgan-Kiss and Cronan 2008; Meng et al. 2018). However, this was not the case

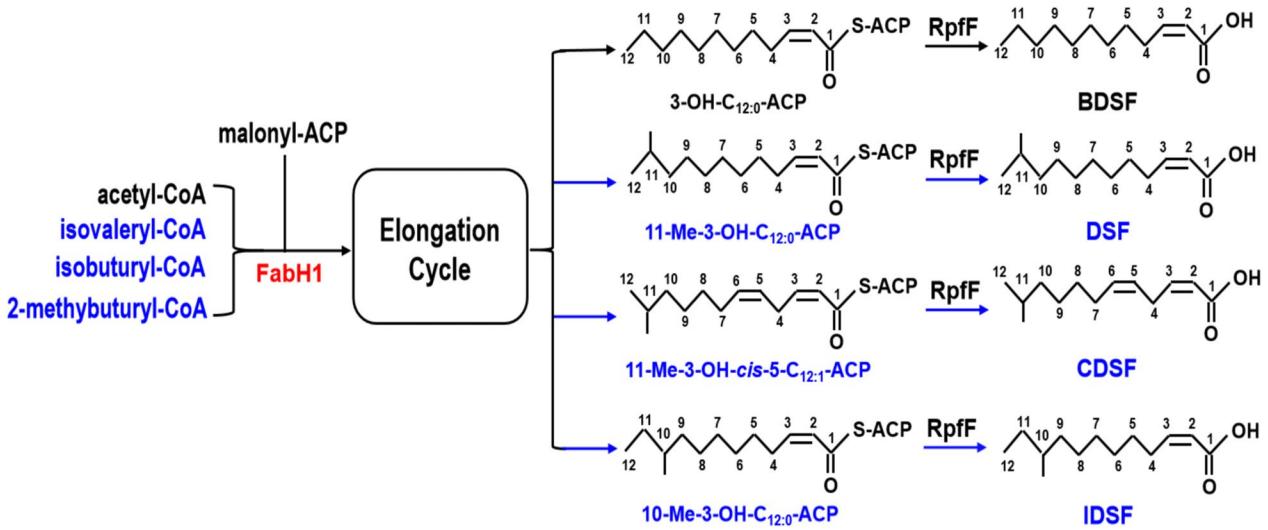

Fig. 6 Schematic biosynthetic pathway of fatty acid and DSF-family signal components in *Xoo*. DSF, *cis*-11-methyl-2-dodecenoic acid; CDSF, *cis*, *cis*-11-methyldodeca-2,5-dienoic acid; IDSF, *cis*-10-methyl-2-dodecenoic acid; BDSF, *cis*-2-dodecenoic acid; FabH1, 3-ketoacyl-ACP synthase III; and RpfF, acyl-ACP thioesterase/dehydratase

in *Xoo*, because the Δ*fabH1* strain grew comparably well to the WT strain, and overexpression of *Xoo fabB* or *fabF* could not rescue the growth of *R. solanacearum* Δ*fabH* (Additional file 1: Figure S3). Based on these results, we speculate that a novel mechanism initiates FAS in *Xoo*, and this is currently being explored in our group.

Conclusions

In this study, we determined that FabH1 is the key enzyme in the production of BCFAs and branched-chain DSF family signal components in *Xoo*, and provided strong evidence that DSF family signal molecules are synthesised via the FAS pathway in *Xanthomonas* species. Pathogenicity analysis showed that loss of *fabH1* caused a significant decrease in the virulence of *Xoo* on rice leaves. Genetic and phenotypic evidence showed that *fabH1* plays a key role in multiple *Xoo* pathogenicity-related functions, including EPS production, biofilm formation, motility, and resistance to environmental stresses.

Methods

Materials

Malonyl-CoA, acetyl-CoA, fatty acids, NADPH, NADH, and antibiotics were purchased from Sigma-Aldrich. Takara Biotechnology Co., Ltd. provided molecular biology reagents. Novagen provided the pET-28(b) vectors. Ni–NTA agarose columns were purchased from Invitrogen. Bio-Rad Co. provided the Quick Start Bradford dye reagent. The oligonucleotide primers were synthesized by Sangon Biotech (Shanghai) Co., Ltd.

Bacterial strains, plasmids, and bacterial growth conditions

The bacterial strains and plasmids are listed in Additional file 2: Table S1. *E. coli* were grown at 37°C in Luria–Bertani medium (yeast extract, 5 g/L; peptone, 10 g/L; NaCl, 10 g/L; pH 7.0) (Hanahan 1983). *Ralstonia solanacearum* strains were grown at 30°C in BG medium (bacto peptone, 10 g/L; yeast extract, 1 g/L; casamino acids, 1 g/L; glucose, 5 g/L; pH 7.0) (Cheng et al. 2012). *Xoo* strains were grown at 30°C in nutrient agar (NA) medium (beef extract, 3 g/L; yeast extract, 1 g/L; peptone, 5 g/L; sucrose, 10 g/L; pH 7.0) (Zhang et al. 2022). The composition of XOLN medium: 0.7 g/L K_2HPO_4, 0.2 g/L KH_2PO_4, 1 g/L $(NH_4)_2SO_4$, 0.1 g/L $MgCl_2$, 0.01 g/L $FeSO_4$, 0.001 g/L $MnCl_2$, 0.0625% tryptone, 0.0625% yeast extract, and 2 g/L sucrose (He et al. 2010). The antibiotics and inducers were added at the concentrations of 30 μg/mL kanamycin sulfate, 30 μg/mL gentamicin, or 30 μg/mL chloramphenicol. Isopropyl-β-D-thiogalactoside (IPTG) was used at a final concentration of 1 mM. Octanoic acid was used at a final concentration of 1 mM.

Complementation of the *R. solanacearum fabH* deletion strain

The *Xoo fabHs* genes were amplified from genomic DNA of *X. oryzae* pv. *oryzae* PXO99A using primers listed in Additional file 2: Table S2. Then the amplified fragment was purified, and inserted into the multicopy plasmid pSRK-Gm (Khan et al. 2008) to generate pMF1 (*fabH1*), pMF2 (*fabH2*), and pMF3 (*fabH3*), respectively. These plasmids were confirmed by nucleotide sequencing performed at Sangon Biotech (Shanghai) Co., Ltd. The derivatives of *E. coli* strain S17-1 carrying these plasmids or empty vector plasmids was mated with *R. solanacearum fabH* deletion strain Δ*RsfabH* (Mao et al. 2015) on BG plates with octanoic acid for 48 h at 30°C. The cells were suspended in BG medium and appropriate dilutions were spread onto BG plates (with octanoic acid) containing chloramphenicol (to select against the donor strain) and gentamicin. The transformed strains were inoculated onto the BG plates with or without octanoic acid, and growth was determined after 2 days incubation at 30°C.

Expression and purification of proteins

pET-28(b) carrying *Xoo fabHs* genes were transformed into BL21 (DE3) cells. The recombinant proteins were then purified using nickel-ion affinity column (Qiagen) following the standard protocol. The purified proteins were examined with SDS-PAGE electrophoresis. The *E. coli* proteins FabD, FabH, FabB, FabG, FabZ, FabI, holo-ACP, and *Vibrio harveyi* AasS proteins were purified as described previously (Zhu et al. 2010).

Assays of 3-ketoacyl-ACP synthase III activity in vitro

The activities of KAS III in the initiation of fatty acid synthesis were assessed with reaction mixtures containing 0.1 M sodium phosphate (pH 7.0), 1 mM β-mercaptoethanol, 0.1 μg each of *E. coli* FabD, FabG, FabA, and FabI, 50 μM holo-ACP, 50 μM NADPH, 50 μM NADH, 100 μM malonyl-CoA, and 100 μM acetyl-CoA ($C_{2:0}$-CoA to $C_{12:0}$-CoA, isobutyryl-CoA, and isovaleryl-CoA) in a final volume of 40 μL. The reactions were initiated by the addition of FabHs to the mixture, followed by incubation for 1 h at 37°C. The resulting products were distinguished with conformationally sensitive gel electrophoresis on 17.5% polyacrylamide gels containing 0.5 M urea optimized for separation (Mao et al. 2015). The gel was stained with InstantBlue Coomassie Protein Stain (Abcam).

Construction of in-frame deletion mutants and complementation

X. oryzae pv. *oryzae* PXO99A was used as the parental strain for the generation of deletion mutants, as

described previously, and the primers used were listed in Additional file 2: Table S2. For single-copy complementation of Δ*fabH1*, the coding region of *fabH1* along with its promoter region was amplified by PCR and was cloned in a versatile mini-*Tn7*T delivery vector mini pUC18-*Tn7*T-Gm plasmid (Choi and Schweizer 2006). The resultant construction was transferred into Δ*fabH1* mutant by electroporation with the helper plasmid pTNS2 and the complementation strain was selected as described previously (Choi and Schweizer 2006).

Analysis of fatty acid profile

To determine fatty acid composition, the strains were grown in BG medium or NA medium to an OD_{600} of 0.6. Cultures were collected by centrifugation and were washed three times with water. Fatty acid methyl esters were generated and extracted and the profile was analyzed by GC–MS as previously described (Yu et al. 2016; Dong et al. 2021).

Pathogenicity assays

The pathogenicity of *Xoo* strains was tested on rice cultivars (*Oryza sativa* L. *japonica* cv. Nipponbare) by leaf-clipping, as previously described (Ray et al. 2000). Briefly, the bacterial were grown in NA medium at 30°C for 2 days, and the cells were washed and resuspended in sterile PBS buffer to an OD_{600} of 0.1. The cells were inoculated on the leaves by leaf-clipping. The lesion length was measured at 2 weeks post inoculation. Twenty leaves for each tested strain were inoculated. Each strain was tested with at least three separated experiments.

Extraction and purification of DSF-family signal components from *Xoo* culture

The method for extraction and purification was described previously (Zhou et al. 2015; Zhou et al. 2017a). To quantify DSF-family signal components production in the culture of the *Xoo* strains by High-performance liquid chromatography (HPLC), *Xoo* strains were cultured in liquid medium for 24 h and 50 mL of the supernatant was collected. The crude ethyl acetate extract was filtered through a 0.45-μm Minisart filter and then concentrated to 0.1 mL for HPLC assays. The extracted matters (20 μL) were examined with a C18 reverse-phase HPLC column (4.6 mm × 250 mm, Agilent Technologies), and were eluted with water: methanol (23:77 v/v, 0.1% formic acid) at a flow rate of 1 mL/min in a Shimadzu prominence LC-20AT system (Shimadzu International Trading Co. Limited) with a UV220 detector. All experiments were repeated three times with similar results.

Motility and biofilm formation assays

The swimming and swarming motility assays were performed on a semi-solid plate containing 0.3% agarose and 0.5% agarose, respectively (Antar et al. 2020). The bacteria of each strain were cultured in NA medium in a shaking incubator at 30°C for 2 days, and the cells were washed and resuspended in water to a final OD_{600} of 2.0. Aliquots (2 μL) of bacteria were spotted onto the swarming plates, and were incubated at 30°C for 3 days, respectively. The assays were repeated at least three times. Biofilm formation assay was described previously (Li and Wang 2012), with slight modifications. The assay was performed by incubating the diluted bacteria inoculated into the borosilicate glass for 7 days at 30°C without shaking. Non-adherent bacteria and medium were removed and washed three times. The attached biofilm was incubated with 0.1% (w/v) crystal violet solution for 30 min at room temperature, and thoroughly washed twice with water and then air-dried. The crystal violet bound cells was solubilized in 90% ethanol and quantified by measuring absorption at 590 nm. The assays were repeated at least three times.

Measurement of the extracellular enzyme activity and EPS production

The activities of extracellular cellulase and amylase were determined on NA plates containing 0.5% (w/v) carboxymethylcellulose (CMC) (for cellulase), 0.2% xylan (for xylanase), and 0.1% (w/v) starch (for amylase), respectively (Wei et al. 2007). Two μL of each *Xoo* strain culture ($OD_{600} \approx 2.0$) was incubated at 30°C for 3 days. The CMC plates were stained with 1% Congo Red solution. The xylanase plates and starch plates were stained with I_2-KI (I_2 at 0.08 mol/L and KI at 3.2 mol/L) solution. The zones of clearance around the spots due to the degradation of the substrate were photographed. The relative activities of the enzymes were indicated by the diameters of the clear zones. Three plates were inoculated in each experiment, and each experiment was repeated three times.

To measure EPS production, each *Xoo* strain culture (1 mL, $OD_{600} \approx 2.0$) was used to inoculate 50 mL of NA liquid medium containing 4% glucose at 30°C for 4 days, with shaking at 180 rpm (Long et al. 2018). EPS was precipitated from the culture supernatant by adding of three volumes of 100% cold ethanol. The precipitated EPS were pelleted by centrifugation at 12,000 *g*, 4°C for 15 min, then air dried and weighed. Three flasks were inoculated in each experiment and were repeated three times.

Effects of environmental factors on the growth of *Xoo*

The bacteria of each strain were cultured in NA medium in a shaking incubator at 30°C for 2 days, and the cells

were washed and resuspended in water to a final OD_{600} of 2.0. Aliquots (5 μL) of bacteria were spotted onto NA plates containing increasing levels of NaCl, SDS, pH, or H_2O_2. All plates were incubated at 30°C for 3 days.

Statistics and reproducibility assays

The experimental datasets were subjected to analyses of variance using GraphPad Prism 8.0. The significance of the treatment effects was determined by the F value ($P=0.05$). If a significant F value was obtained, separation of means was accomplished by Fisher's protected least significant difference at $P \leq 0.05$.

Abbreviations

Acetyl-CoA	Acetyl coenzyme A
ACP	Acyl carrier protein
AHL	*N*-Acyl-homoserine lactones
BCFAs	Branched-chain fatty acids
BDSF	*cis*-2-Dodecenoic acid
CDSF	*cis*, *cis*-11-Methyldodeca-2, 5-dienoic acid
DSF	*cis*-11-Methyl-2-dodecenoic acid
FabB	3-Ketoacyl ACP synthase I
FabF	3-Ketoacyl ACP synthase II
FabH	3-Ketoacyl ACP synthase III
FAS	Fatty acid synthesis
GC–MS	Gas chromatography–mass spectrometry
HPLC	High-performance liquid chromatography
IDSF	*cis*-10-Methyl-2-dodecenoic acid
KASIII	3-Ketoacyl ACP synthase III
Malonyl-ACP	Malonyl-acyl carrier protein
SCFAs	Straight-chain fatty acids

Supplementary Information

The online version contains supplementary material available at https://doi.org/10.1186/s42483-023-00180-2.

Additional file 1: **Figure S1**. FabH2 and FabH3 failed to catalyze the elongation of the acyl-CoAs and branched-chain acyl-CoAs. **Figure S2**. Growth curves of Xoo fabHs deletion mutations at 30°C in NAand XOL-Nmedia. **Figure S3**. XoofabB and XoofabF could not restore the growth of R. solanacearum fabH knockout strain ΔRsfabH on BG medium in the absence of octanoic acid.

Additional file 2: **Table S1**. Bacterial strains and plasmids used in this study. **Table S2**. Sequences of the PCR primers used in this study.

Acknowledgements

Not applicable.

Authors' contributions

HW and MY conceived and designed the project. MY, LL, and YY carried out the experiments. MY, MH, JS, WZ, and YZ provided the resources and analyzed the data. HW, ZH, YY, and JM wrote the manuscript. All authors read and approved the final manuscript.

Funding

This study was supported by the National Natural Science Foundation of China (Grants 31671987 and 31972232), the Natural Science Foundation of Guangdong Province (Grant 2021A1515110166), the Double First-class Discipline Promotion Project (Grant 2021B10564001), the International Science and Technology Program of Guangdong (Grant 2022A0505050060), the Characteristic Innovation Project of Colleges and Universities in Guangdong Province (Grant 2022KTSCX271), and the Science Foundation of Guangdong Food & Drug Vocational College (Grant 2020ZR03).

Availability of data and materials

The data that support the findings of this study are available from the corresponding author upon reasonable request.

Declarations

Ethics approval and consent to participate

Not applicable.

Consent for publication

Not applicable.

Competing interests

The authors declare that they have no competing interests.

Received: 1 January 2023 Accepted: 22 May 2023
Published online: 13 June 2023

References

An SQ, Allan JH, McCarthy Y, Febrer M, Dow JM, Ryan RP. The PAS domain-containing histidine kinase RpfS is a second sensor for the diffusible signal factor of *Xanthomonas campestris*. Mol Microbiol. 2014;92:586–97. https://doi.org/10.1111/mmi.12577.

Andrade MO, Alegria MC, Guzzo CR, Docena C, Rosa MC, Ramos CH, et al. The HD-GYP domain of RpfG mediates a direct linkage between the Rpf quorum-sensing pathway and a subset of diguanylate cyclase proteins in the phytopathogen *Xanthomonas axonopodis* pv. *citri*. Mol Microbiol. 2006;62:537–51. https://doi.org/10.1111/j.1365-2958.2006.05386.x.

Antar A, Lee MA, Yoo Y, Cho MH, Lee SW. PXO_RS20535, encoding a novel response regulator, is required for chemotactic motility, biofilm formation, and tolerance to oxidative stress in *Xanthomonas oryzae* pv. *oryzae*. Pathogens. 2020. https://doi.org/10.3390/pathogens9110956.

Bi H, Yu Y, Dong H, Wang H, Cronan JE. *Xanthomonas campestris* RpfB is a fatty Acyl-CoA ligase required to counteract the thioesterase activity of the RpfF diffusible signal factor (DSF) synthase. Mol Microbiol. 2014;93:262–75. https://doi.org/10.1111/mmi.12657.

Campbell JW, Cronan JE Jr. Bacterial fatty acid biosynthesis: targets for antibacterial drug discovery. Annu Rev Microbiol. 2001;55:305–32. https://doi.org/10.1146/annurev.micro.55.1.305.

Cheng J, Ma J, Lin J, Fan ZC, Cronan JE, Wang H. Only one of the five *Ralstonia solanacearum* long-chain 3-ketoacyl-acyl carrier protein synthase homologues functions in fatty acid synthesis. Appl Environ Microbiol. 2012;78:1563–73. https://doi.org/10.1128/AEM.07335-11.

Choi KH, Schweizer HP. mini-Tn7 insertion in bacteria with single attTn7 sites: example *Pseudomonas aeruginosa*. Nat Protoc. 2006;1:153–61. https://doi.org/10.1038/nprot.2006.24.

Choi KH, Heath RJ, Rock CO. beta-ketoacyl-acyl carrier protein synthase III (FabH) is a determining factor in branched-chain fatty acid biosynthesis. J Bacteriol. 2000;182:365–70. https://doi.org/10.1128/JB.182.2.365-370.2000.

Cronan JE Jr. Rock CO: biosynthesis of membrane lipids. EcoSal plus. 2008. https://doi.org/10.1128/ecosalplus.3.6.4.

Cronan JE, Zhao X, Jiang Y. Function, attachment and synthesis of lipoic acid in *Escherichia coli*. Adv Microb Physiol. 2005;50:103–46. https://doi.org/10.1016/S0065-2911(05)50003-1.

Davis MS, Solbiati J, Cronan JE Jr. Overproduction of acetyl-CoA carboxylase activity increases the rate of fatty acid biosynthesis in *Escherichia coli*. J Biol Chem. 2000;275:28593–8. https://doi.org/10.1074/jbc.M004756200.

Dong H, Ma J, Chen Q, Chen B, Liang L, Liao Y, et al. A cryptic long-chain 3-ketoacyl-ACP synthase in the *Pseudomonas putida* F1 unsaturated fatty acid synthesis pathway. J Biol Chem. 2021;297:100920. https://doi.org/10.1016/j.jbc.2021.100920.

Du J, Zhang A, Hao J, Wang J. Biosynthesis of di-rhamnolipids and variations of congeners composition in genetically-engineered

Escherichia coli. Biotechnol Lett. 2017;39:1041–8. https://doi.org/10.1007/s10529-017-2333-2.
Hanahan D. Studies on transformation of *Escherichia coli* with plasmids. J Mol Biol. 1983;166:557–80. https://doi.org/10.1016/s0022-2836(83)80284-8.
He YW, Zhang LH. Quorum sensing and virulence regulation in *Xanthomonas campestris*. FEMS Microbiol Rev. 2008;32:842–57. https://doi.org/10.1111/j.1574-6976.2008.00120.x.
He YW, Wu J, Cha JS, Zhang LH. Rice bacterial blight pathogen *Xanthomonas oryzae* pv. *oryzae* produces multiple DSF-family signals in regulation of virulence factor production. BMC Microbiol. 2010;10:187. https://doi.org/10.1186/1471-2180-10-187.
Heath RJ, Rock CO. Regulation of malonyl-CoA metabolism by acyl-acyl carrier protein and beta-ketoacyl-acyl carrier protein synthases in *Escherichia coli*. J Biol Chem. 1995;270:15531–8. https://doi.org/10.1074/jbc.270.26.15531.
Heath RJ, White SW, Rock CO. Lipid biosynthesis as a target for antibacterial agents. Prog Lipid Res. 2001;40:467–97. https://doi.org/10.1016/s0163-7827(01)00012-1.
Huang YH, Lin JS, Ma JC, Wang HH. Functional characterization of triclosan-resistant enoyl-acyl-carrier protein reductase (FabV) in *Pseudomonas aeruginosa*. Front Microbiol. 2016;7:1903. https://doi.org/10.3389/fmicb.2016.01903.
Khan SR, Gaines J, Roop RMII, Farrand SK. Broad-host-range expression vectors with tightly regulated promoters and their use to examine the influence of TraR and TraM expression on Ti plasmid quorum sensing. Appl Environ Microbiol. 2008;74:5053–62. https://doi.org/10.1128/AEM.01098-08.
Lai CY, Cronan JE. Beta-ketoacyl-acyl carrier protein synthase III (FabH) is essential for bacterial fatty acid synthesis. J Biol Chem. 2003;278:51494–503. https://doi.org/10.1074/jbc.M308638200.
Li J, Wang N. The gpsX gene encoding a glycosyltransferase is important for polysaccharide production and required for full virulence in *Xanthomonas citri* subsp. *citri*. BMC Microbiol. 2012;12:31. https://doi.org/10.1186/1471-2180-12-31.
Li Y, Florova G, Reynolds KA. Alteration of the fatty acid profile of *Streptomyces coelicolor* by replacement of the initiation enzyme 3-ketoacyl acyl carrier protein synthase III (FabH). J Bacteriol. 2005;187:3795–9. https://doi.org/10.1128/JB.187.11.3795-3799.2005.
Lin S, Cronan JE. Closing in on complete pathways of biotin biosynthesis. Mol Biosyst. 2011;7:1811–21. https://doi.org/10.1039/c1mb05022b.
Long JY, Song KL, He X, Zhang B, Cui XF, Song CF. Mutagenesis of PhaR, a regulator gene of polyhydroxyalkanoate biosynthesis of *Xanthomonas oryzae* pv. *oryzae* caused pleiotropic phenotype changes. Front Microbiol. 2018;9:3046. https://doi.org/10.3389/fmicb.2018.03046.
Magnuson K, Oh W, Larson TJ, Cronan JE Jr. Cloning and nucleotide sequence of the *fabD* gene encoding malonyl coenzyme A-acyl carrier protein transacylase of *Escherichia coli*. FEBS Lett. 1992;299:262–6. https://doi.org/10.1016/0014-5793(92)80128-4.
Mansfield J, Genin S, Magori S, Citovsky V, Sriariyanum M, Ronald P, et al. Top 10 plant pathogenic bacteria in molecular plant pathology. Mol Plant Pathol. 2012;13:614–29. https://doi.org/10.1111/j.1364-3703.2012.00804.x.
Mao YH, Ma JC, Li F, Hu Z, Wang HH. *Ralstonia solanacearum* RSp0194 encodes a novel 3-keto-acyl carrier protein synthase III. PLoS ONE. 2015;10:e0136261. https://doi.org/10.1371/journal.pone.0136261.
Marrakchi H, Zhang YM, Rock CO. Mechanistic diversity and regulation of Type II fatty acid synthesis. Biochem Soc Trans. 2002;30:1050–5. https://doi.org/10.1042/bst0301050.
Meng Q, Liang H, Gao H. Roles of multiple KASIII homologues of *Shewanella oneidensis* in initiation of fatty acid synthesis and in cerulenin resistance. Biochim Biophys Acta Mol Cell Biol Lipids. 2018;1863:1153–63. https://doi.org/10.1016/j.bbalip.2018.06.020.
Morgan-Kiss RM, Cronan JE. The *Lactococcus lactis* FabF fatty acid synthetic enzyme can functionally replace both the FabB and FabF proteins of *Escherichia coli* and the FabH protein of *Lactococcus lactis*. Arch Microbiol. 2008;190:427–37. https://doi.org/10.1007/s00203-008-0390-6.
Nino-Liu DO, Ronald PC, Bogdanove AJ. *Xanthomonas oryzae* pathovars: model pathogens of a model crop. Mol Plant Pathol. 2006;7:303–24. https://doi.org/10.1111/j.1364-3703.2006.00344.x.
Parsons JB, Rock CO. Bacterial lipids: metabolism and membrane homeostasis. Prog Lipid Res. 2013;52:249–76. https://doi.org/10.1016/j.plipres.2013.02.002.
Rai R, Ranjan M, Pradhan BB, Chatterjee S. Atypical regulation of virulence-associated functions by a diffusible signal factor in *Xanthomonas oryzae* pv. *oryzae*. Mol Plant Microbe Interact. 2012;25:789–801. https://doi.org/10.1094/MPMI-11-11-0285-R.
Ray SK, Rajeshwari R, Sonti RV. Mutants of *Xanthomonas oryzae* pv. *oryzae* deficient in general secretory pathway are virulence deficient and unable to secrete xylanase. Mol Plant Microbe Interact. 2000;13:394–401. https://doi.org/10.1094/MPMI.2000.13.4.394.
Singh AK, Zhang YM, Zhu K, Subramanian C, Li Z, Jayaswal RK, et al. FabH selectivity for anteiso branched-chain fatty acid precursors in low-temperature adaptation in *Listeria monocytogenes*. FEMS Microbiol Lett. 2009;301:188–92. https://doi.org/10.1111/j.1574-6968.2009.01814.x.
Slater H, Alvarez-Morales A, Barber CE, Daniels MJ, Dow JM. A two-component system involving an HD-GYP domain protein links cell-cell signalling to pathogenicity gene expression in *Xanthomonas campestris*. Mol Microbiol. 2000;38:986–1003. https://doi.org/10.1046/j.1365-2958.2000.02196.x.
Torres PS, Malamud F, Rigano LA, Russo DM, Marano MR, Castagnaro AP, et al. Controlled synthesis of the DSF cell-cell signal is required for biofilm formation and virulence in *Xanthomonas campestris*. Environ Microbiol. 2007;9:2101–9. https://doi.org/10.1111/j.1462-2920.2007.01332.x.
Vauterin L, Yang P, Swings J. Utilization of fatty acid methyl esters for the differentiation of new *Xanthomonas* species. Int J Syst Bacteriol. 1996;46:298–304. https://doi.org/10.1099/00207713-46-1-298.
Wang XY, Zhou L, Yang J, Ji GH, He YW. The RpfB-dependent quorum sensing signal turnover system is required for adaptation and virulence in rice bacterial blight pathogen *Xanthomonas oryzae* pv. *oryzae*. Mol Plant Microbe Interact. 2016;29:220–30. https://doi.org/10.1094/MPMI-09-15-0206-R.
Wei K, Tang DJ, He YQ, Feng JX, Jiang BL, Lu GT, et al. *hpaR*, a putative marR family transcriptional regulator, is positively controlled by HrpG and HrpX and involved in the pathogenesis, hypersensitive response, and extracellular protease production of *Xanthomonas campestris* pathovar *campestris*. J Bacteriol. 2007;189:2055–62. https://doi.org/10.1128/JB.01331-06.
White SW, Zheng J, Zhang YM, Rock CO. The structural biology of type II fatty acid biosynthesis. Annu Rev Biochem. 2005;74:791–831. https://doi.org/10.1146/annurev.biochem.74.082803.133524.
Yu YH, Hu Z, Dong HJ, Ma JC, Wang HH. *Xanthomonas campestris* FabH is required for branched-chain fatty acid and DSF-family quorum sensing signal biosynthesis. Sci Rep. 2016;6:32811. https://doi.org/10.1038/srep32811.
Zhang YM, Rock CO. Membrane lipid homeostasis in bacteria. Nat Rev Microbiol. 2008;6:222–33. https://doi.org/10.1038/nrmicro1839.
Zhang YQ, Zhang S, Sun /ML, Su HN, Li HY, Kun L, et al. Antibacterial activity of peptaibols from Trichoderma longibrachiatum SMF2 against gram-negative *Xanthomonas oryzae* pv. *oryzae*, the causal agent of bacterial leaf blight on rice. Front Microbiol. 2022;13:1034779. https://doi.org/10.3389/fmicb.2022.1034779.
Zhou L, Yu Y, Chen X, Diab AA, Ruan L, He J, et al. The multiple DSF-family QS signals are synthesized from carbohydrate and branched-chain amino acids via the FAS elongation cycle. Sci Rep. 2015;5:13294. https://doi.org/10.1038/srep13294.
Zhou L, Wang XY, Zhang W, Sun S, He YW. Extraction, purification and quantification of diffusible signal factor family quorum-sensing signal molecules in *Xanthomonas oryzae* pv. *oryzae*. Bio Protoc. 2017a;7:2190. https://doi.org/10.21769/BioProtoc.2190.
Zhou L, Zhang LH, Camara M, He YW. The DSF family of quorum sensing signals: diversity, biosynthesis, and turnover. Trends Microbiol. 2017b;25:293–303. https://doi.org/10.1016/j.tim.2016.11.013.
Zhu L, Lin J, Ma J, Cronan JE, Wang H. Triclosan resistance of *Pseudomonas aeruginosa* PAO1 is due to FabV, a triclosan-resistant enoyl-acyl carrier protein reductase. Antimicrob Agents Chemother. 2010;54:689–98. https://doi.org/10.1128/AAC.01152-09.
Zhu PL, Zhao S, Tang JL, Feng JX. The rsmA-like gene *rsmA* (*Xoo*) of *Xanthomonas oryzae* pv. *oryzae* regulates bacterial virulence and production of diffusible signal factor. Mol Plant Pathol. 2011;12:227–37. https://doi.org/10.1111/j.1364-3703.2010.00661.x.